THE JOURNAL OF PHYSICAL CHEMISTRY A

Article

pubs.acs.org/JPCA

Electronic Structure and Thermochemical Parameters of the Silicon-Doped Boron Clusters B_nSi, with n = 8−14, and Their Anions

Dang Thi Tuyet Mai,[†] Long Van Duong,[‡] Truong Ba Tai,[†] and Minh Tho Nguyen*[,†]

[†]Department of Chemistry, KU Leuven, Celestijnenlaan 200F, B-3001 Leuven, Belgium

[‡]Institute for Computational Science and Technology (ICST), Quang Trung Software City, Ho Chi Minh City, Viet Nam

Supporting Information

ABSTRACT: We performed a systematic investigation on silicon-doped boron clusters B_nSi (n = 8−14) in both neutral and anionic states using quantum chemical methods. Thermochemical properties of the lowest-lying isomers of $B_nSi^{0/-}$ clusters such as total atomization energies, heats of formation at 0 and 298 K, average binding energies, dissociation energies, etc. were evaluated by using the composite G4 method. The growth pattern for $B_nSi^{0/-}$ with n = 8−14 is established as follows: (i) $B_nSi^{0/-}$ clusters tend to be constructed by substituting B atom by Si-atom or adding one Si-impurity into the parent B_n clusters with n to be even number, and (ii) Si favors an external position of the B_n frameworks. Our theoretical results reveal that B_8Si, B_9Si^-, $B_{10}Si$ and $B_{13}Si^-$ are systems with enhanced stability due to having high average binding energies, second-order difference in energies and dissociation energies. Especially, by analyzing the MOs, ELF, and ring current maps, the enhanced stability of B_8Si can be rationalized in terms of a triple aromaticity.

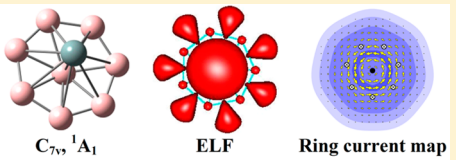

Structure and chemical bonding of B_8Si

1. INTRODUCTION

During the past several decades, boron-based compounds have been attracting considerable interest, in part due to their remarkable properties as well as their potentially useful applications. With the sp^2 hybridization of the valence electrons, the short covalent radius, the electron deficiency, and the unique molecular architecture, both organic and inorganic boron based compounds have been studied, which has led to practical applications in many fields such as medicine, the oil industry, and materials.[1−4] A large number of investigations on boron clusters, and their derivatives doped by other elements, have been also reported.[5−11] Recent studies showed that the stability of tubular forms of B_{14}, B_{16} and the fullerene forms of B_{18}, B_{20} can be enhanced by doping by a transition metal such as Fe.[12] The systematic investigations on small and singly doped B_nM clusters with n up to 12, where M are transition metals or metals such as Sc, Zr, Al, have been studied theoretically[13−15] and experimentally.[16−20] The nature of bonding and origin of stability in the doubly metal doped boron clusters B_nM_2 (M = Co, Fe)[21] and the electronic structure of mixed clusters, such as the Mg_nB_m clusters ($1 \le n \le 15$, $0 \le m \le 3$) in which boron plays the role of dopant,[22] were analyzed in details.

Of the binary boron compounds, the boron−silicon systems have been the subject of extensive theoretical and experimental studies.[23−31] Zaitsev et al.[32] used Knudsen effusion mass spectrometry to investigate thermodynamic properties of Si−B alloys in which boron content is from 1.5 up to 100 at %. By using band calculations with pseudopotential method, electronic densities of states of β-B, B_nSi, B_6Si and B_3Si or B_4Si were calculated by Imai et al.[33] Recently, some of us systematically investigated singly boron-doped silicon clusters Si_nB (n = 1−10) in various charge states (−1; 0; +1) using the G4 and CCSD(T) methods.[34] The growth mechanism of the Si_nB clusters has been established, in which the attachment of one Si atom into the smaller-sized $Si_{n-1}B$ is preferred over that by the addition of a B atom into the pure Si_n clusters. Nevertheless, both systems B_nSi and BSi_n have only the dimer BSi in common, and they grow up following quite different patterns.

Although the importance of the boron−silicon compounds is demonstrated, an understanding of their geometric and electronic structure and a reliable determination of their thermodynamic properties is still limited. According to the best of our knowledge, only a few studies on small B_nSi clusters have been performed. Viswanathan et al.[35] measured the heats of formation of BSi, BSi_2, and BSi_3 in the gas phase. A theoretical study on structure, energies, and vibrational spectra of B_2Si, BSi_2, and B_2Si_2 using molecular orbital (MO) calculations was also reported by Davy et al.[36] More recently, by applying density functional (DFT) and coupled-cluster (CCSD(T)) theories for a systematic investigation on the small-size $B_nSi^{0/-}$ clusters with n = 1−7, Tai et al.[37] predicted, among other properties, that the first three-dimensional (3D) global minimum is already located at the B_7Si size. The larger sizes of B_nSi clusters with n > 7 have however not been examined yet. In this context, some intriguing questions arise: are the global minima of the B_nSi systems with n > 7 still 3D structures, and does the growth mechanism of the larger size B_nSi clusters involve some (quasi)-planar structures as in the case of pure

Received: January 26, 2016
Revised: April 26, 2016
Published: April 29, 2016

DOI: 10.1021/acs.jpca.6b00847
J. Phys. Chem. A 2016, 120, 3623−3633

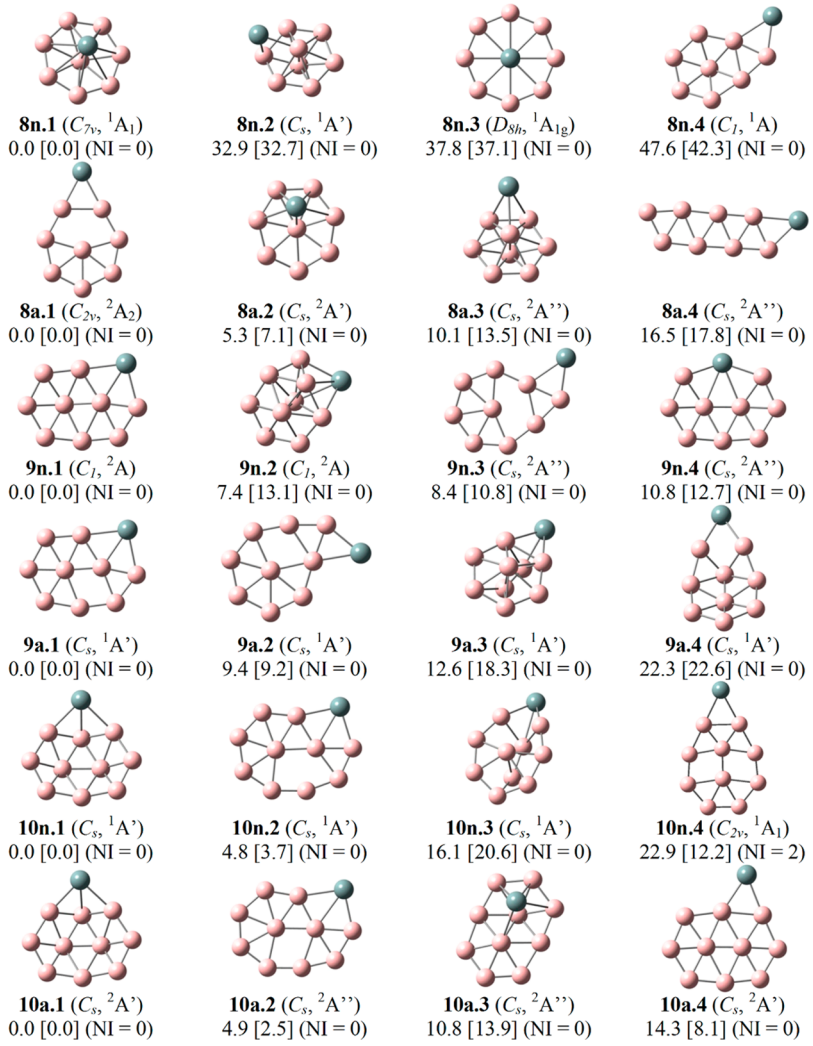

Figure 1. Shapes, symmetries, relative energies (ΔE, kcal/mol), and number of imaginary frequencies (NI) of the lower-lying structures of B_nSi and B_nSi^- (n = 8−10) using the G4 method. Values given in brackets are from PBE/6-311+G(d) + ZPE computations.

boron clusters? Motivated by these issues and in relation to our recent theoretical studies on binary boron−silicon compounds, we set out to investigate systematically on a series of the silicon-doped boron clusters B_nSi in the following sizes, namely with n = 8−14, in both the neutral and anionic states. Together with the geometrical aspects, we then discuss their electronic structures, chemical bonding, growth behavior, and thermochemical properties by predicting their heats of formation, average binding energies and dissociation energies using reliable quantum chemical methods.

2. COMPUTATIONAL METHODS

The initial search for all possible lower-lying isomers of each B_nSi size was carried out by using a stochastic search algorithm that was implemented by our group.[38] First, the possible structures were generated by a random kick method, and then rapidly optimized using density functional theory (DFT) with the PBE functional in conjunction with the 6-31G(d) basis set.[39,40] In addition, another series of initial structures of B_nSi were also manually constructed by either adding one Si-atom into the pure B_n clusters at various positions or replacing one B atom of the B_{n+1} parents by one Si-atom. Geometries and harmonic vibrational frequencies of the lower-lying isomers B_nSi and their anions with relative energies of <5.0 eV with respect to the corresponding lowest-lying isomer were recalculated using the PBE functional but with the larger 6-311+G(d) basis set.[41] In order to determine the global minima of clusters considered, the lowest-lying isomers obtained at the latter level were refined at higher level of theory by using the composite G4 approach.[42] Let us note that in the composite G4 procedure, molecular geometries are optimized using the B3LYP functional with the 6-31+G(2df) basis set. In general, the geometries obtained for the lowest-lying isomers are quite similar, when using both PBE and B3LYP functionals. When an energy ordering change occurs in going from DFT to the G4 level, it is due to the difference between DFT and CCSD(T) (of the G4) electronic energies.

The shapes, relative energies given in kcal/mol, symmetrical point group, and number of imaginary frequencies of the neutral B_nSi and anionic B_nSi^- clusters are predicted in Figures 1, 2, and 3. As for a convention, each structure considered hereafter is labeled by ***n*X.Y** in which ***n*** is the number of B atoms, **X** = **n** or **a** stands for a neutral or anionic form, respectively, and **Y** = **1**, **2**... indicates the order of isomers in terms of stability. The structure ***n*X.1** consistently corresponds to the lowest-lying isomer (0 kcal/mol references).

Enthalpies of formation at 0 and 298 K of the global minima can thus obtained from their corresponding total atomization

DOI: 10.1021/acs.jpca.6b00847
J. Phys. Chem. A 2016, 120, 3623−3633

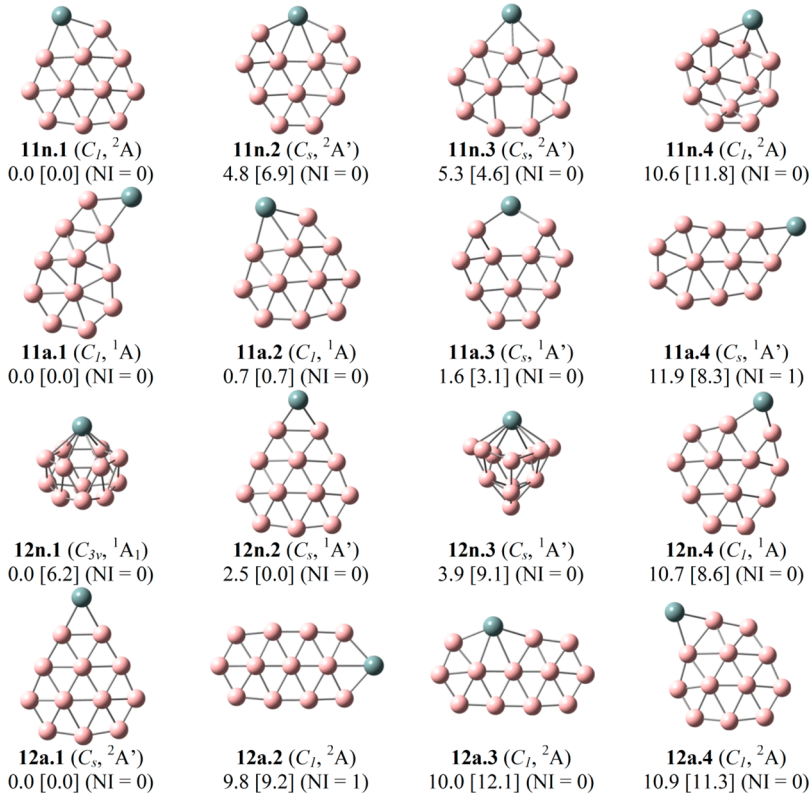

Figure 2. Shapes, symmetries, relative energies (ΔE, kcal/mol), and number of imaginary frequencies (NI) of the lower-lying structures of B_nSi and B_nSi^- (n = 11−12) using the G4 method. Values given in brackets are from PBE/6-311+G(d) + ZPE computations.

energies (TAE)[43] on the basis of the G4 energies. This approach was effectively used for the series of small silicon-doped boron clusters B_nSi with n = 1−7,[37] whose experimental heats of formation of a few clusters are available. From the combination of computed TAE values with the known experimental heats of formation at 0 K for the elements B and Si, $\Delta H_f°$ values at 0 K for the molecules were derived in the gas phase. In this study, we use the values $\Delta H_f°$(B) = 135.1 ± 0.2 kcal/mol, and $\Delta H_f°$(Si) = 107.2 ± 0.2 kcal/mol.[44] The heats of formation at 298 K were calculated by following the classical thermochemical procedure.[45] Other energetic properties such as average binding energy, adiabatic detachment energy, and dissociation energy were also computed from the G4 total energies. The calculated results for thermochemical parameters are summarized in Table 1.

Chemical bonding and the aromatic character[46] were subsequently examined using the topological analysis of the canonical MOs and electron localization function (ELF),[47,48] as well as the magnetic ring current approach.[49,50] Calculations of the magnetic responses and ring currents were performed using the Gamess-UK program[51,52] in conjunction with the SYSMO package.[53] All standard electronic structure calculations were carried out using the Gaussian 09 set of programs.[54]

3. RESULTS AND DISCUSSION

3.1. Electronic Structure of the Clusters B_nSi and B_nSi^- and Their Growth Mechanism. Let us first briefly describe the geometries, electronic structures and relative stabilities of the clusters considered. The relative energies between isomers mentioned in the following sections are obtained from G4 computations.

B_8Si and B_8Si^-. In agreement with a previous study,[56] our calculated results point out that a high symmetry form **8n.1** (C_{7v}, ^{1}A$_1$) in which one B atom of the heptagonal bipyramid D_{7h} B_9 cluster[55] is substituted by a Si atom, is found to be the global minimum of the neutral B_8Si. This structure is similar to the ground state of B_8Al,[8] B_8Li,[57] and also B_8Sc.[13] The second lowest-lying isomer **8n.2** (C_s, ^{1}A′) is formed by adding one Si atom into the hexagonal bipyramid B_8 framework with relative energy of 33 kcal/mol. The next low-lying isomers are a wheel-like structure **8n.3** (D_{8h}, ^{1}A$_{1g}$) constructed by replacing the centered-boron atom of B_9 wheel[58] with Si and a quasi-planar geometry **8n.4** (C_1, ^{1}A), which are 38 and 48 kcal/mol above the heptagonal bipyramid **8n.1**, respectively.

In the anionic state, in the most stable form of B_8Si^-, the planar structure **8a.1** (C_{2v}, ^{2}A$_2$), one B atom on the apex of the B_9^+ cluster[58] is replaced by a Si atom. The second isomer **8a.2** (C_s, ^{2}A′), which is distorted from the high symmetry **8n.1**, has a relative energy of 5 kcal/mol. The **8a.3** (C_s, ^{2}A″) possesses a similar shape as the second-lying isomer **8n.2** of the neutral B_8Si, being 10 kcal/mol above **8a.1**. The double-chain quasi-planar "ribbon" **8a.4** (C_s, ^{2}A″), which is about 17 kcal/mol higher in energy with respect to **8a.1**, is generated by connecting single Si at the peripheral position of the zigzag B_8 form.

B_9Si and B_9Si^-. In the ground state structure **9n.1** (C_1, ^{2}A), a peripheral B atom of the B_{10} skeleton[55] is substituted by Si impurity. The nonsymmetrical 3D form **9n.2** (C_1, ^{2}A) is located within about 7 kcal/mol above **9n.1**. An addition of one Si-atom into the external position of the B_9^+ cluster[58] gives rise to the third-lying isomer **9n.3** (C_s, ^{2}A″) with an energy separation of 8 kcal/mol. Being constructed with the same motif as with **9n.1** but at another peripheral position of the B_{10} framework,[55]

DOI: 10.1021/acs.jpca.6b00847
J. Phys. Chem. A 2016, 120, 3623−3633

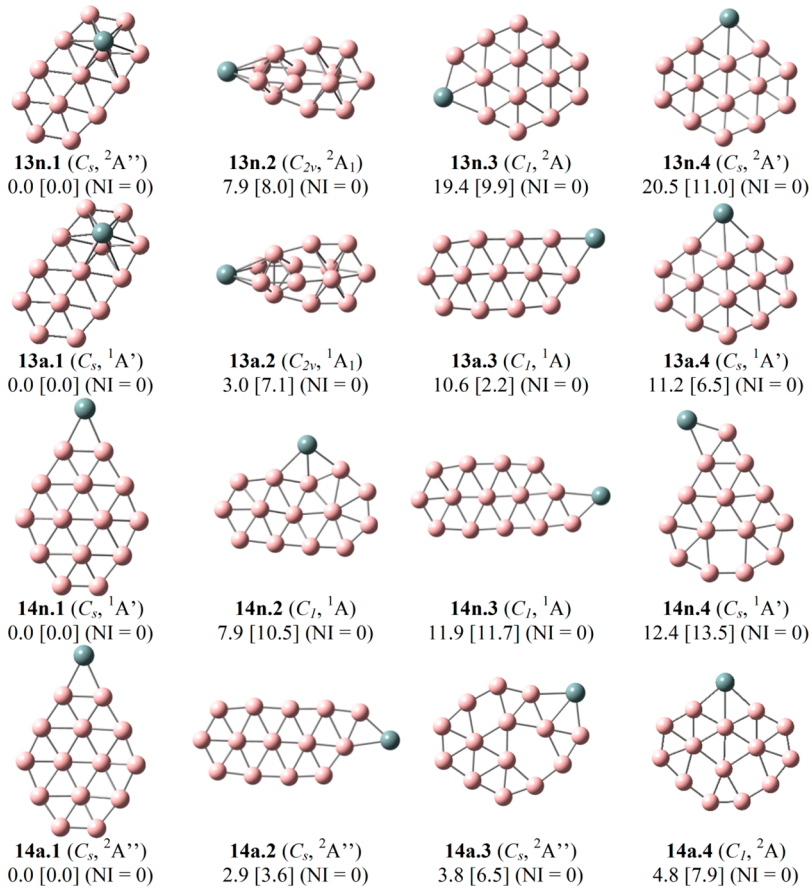

Figure 3. Shapes, symmetries, relative energies (ΔE, kcal/mol), and number of imaginary frequencies (NI) of the lower-lying structures of B_nSi and B_nSi^- (n = 13−14) using the G4 method. Values given in brackets are from PBE/6-311+G(d) + ZPE computations.

Table 1. Average Binding Energies (E_b, eV) (G4 Approach) and HOMO−LUMO Gaps (HLG, eV) of $B_nSi^{0/-}$ Clusters (PBE/6-311+G(d))

neutrals	E_b	HLG	anions	E_b	HLG
8n.1	4.49	4.34	**8a.1**	4.49	-
9n.1	4.40	-	**9a.1**	4.62	0.88
10n.1	4.51	1.91	**10a.1**	4.61	-
11n.1	4.52	-	**11a.1**	4.66	1.41
12n.1	4.59	2.21	**12a.1**	4.70	-
13n.1	4.65	-	**13a.1**	4.78	0.61
14n.1	4.66	1.28	**14a.1**	4.77	-

9n.4 (C_s, ^{2}A″) is the next isomer with relative energy of 11 kcal/mol.

Following attachment of one excess electron, the geometries of two corresponding anions **9a.1** and **9a.2** retain the structures of their neutral counterparts with slight distortions. Consequently, **9a.1** (C_s, ^{1}A′) is also the global minima of the anionic cluster B_9Si^-, and **9a.2** (C_s, ^{1}A′), which corresponds to the anion of **9n.3**, is the second-lying isomer with an energy interval of 9 kcal/mol. The next stable isomers include two C_s structures **9a.3** and **9a.4**, in which Si-atom prefers to be added into the B_9 host at the external position, with a relative energy of 13 and 22 kcal/mol, respectively.

$B_{10}Si$ and $B_{10}Si^-$. Our calculations predict that **10n.1** (C_s, ^{1}A′) is constructed by adding one Si-atom into the B_{10} framework[55] at the external position. The second lowest-lying isomer **10n.2** (C_s, ^{1}A′) is formed by substituting a peripheral B atom of the B_{11} host[55] by a Si impurity with an energy gap of 5 kcal/mol. Considerably, the second stable geometry **10n.2** derived in this work possesses the same shape with the ground state of $B_{10}Al$.[8] A 3D configuration **10n.3** (C_s, ^{1}A′) and a planar structure **10n.4** (C_{2v}, ^{1}A$_1$) with two imaginary frequencies (NI = 2) are found to be the next isomers with relative energy of 16 and 23 kcal/mol, respectively.

Similar to B_9Si^-, the two corresponding anions **10a.1** and **10a.2** continue to keep the geometries of their neutral counterparts following attaching one excess electron. Specifically, **10a.1** (C_s, ^{2}A′) and **10a.2** (C_s, ^{2}A″) turn out to be the two lowest-lying minima of the anionic clusters $B_{10}Si^-$ with an energy separation of 5 kcal/mol. Based on the pure B_{10}^- skeleton,[55] the third-lying isomer **10a.3** (C_s, ^{2}A″) is generated by adding a single Si atom to form a hexagonal bipyramid with around 11 kcal/mol in energy above **10a.1**. The structure **10a.3** (C_s, ^{2}A′), which is distorted from **10a.1**, is the next isomer, being 14 kcal/mol less stable than **10a.1**.

$B_{11}Si$ and $B_{11}Si^-$. Our results show that replacement of one peripheral B atom at various external positions of the B_{12} cluster[55,59] by a Si-atom constructs the ground state configuration **11n.1** (C_1, ^{2}A) and the second one **11n.2** (C_s, ^{2}A′) of the $B_{11}Si$ cluster with an energy interval of about 5 kcal/mol. Differently, doping a Si impurity into the B_{11} host[55] generates the third stable form **11n.3** (C_s, ^{2}A′) with relative energy of also 5 kcal/mol. It is worth noting that the structure **11n.3** is the lowest-lying isomer of the $B_{11}Al$ counterpart.[8] A low symmetry bowl **11n.4** (C_1, ^{2}A) is also located as a local

DOI: 10.1021/acs.jpca.6b00847
J. Phys. Chem. A 2016, 120, 3623−3633

minimum being 11 kcal/mol higher in energy as compared to **11n.1**.

There is a structural competition to be the lowest-lying isomer for $B_{11}Si^-$. Accordingly, two low symmetry structures (C_1, ^1A) including **11a.1** in which Si-atom bridges with its two B neighbors at the external position of B_{11}, and **11a.2**, which is actually the anionic state of **11n.1**, are almost degenerate within an energy gap of 1 kcal/mol. The next isomers include **11a.3** (C_s, $^1A'$), which corresponds to an anionic minimum of **11n.2**, and a planar **11a.4** (C_s, $^1A'$), which is a transition state (NI = 1) with relative energy of 2 and 12 kcal/mol, respectively.

$B_{12}Si$ and $B_{12}Si^-$. At the PBE/6-311+G(d) level, the most stable form of $B_{12}Si$ is a low symmetry structure **12n.2** (C_s, $^1A'$), which is derived by adding the Si atom to connect with two-boron edge of the B_{12} skeleton.[55,59] The second-lying isomer turns out to be a double-hexagonal pyramid **12n.1** (C_{3v}, $^1A_1$) in which Si is located at the top of the pyramid. However, G4 calculations reveal a reversed energy ordering that the pyramid **12n.1** is now the global minimum with a small energy gap of 3 kcal/mol below **12n.2**. The next structure **12n.3** (C_s, $^1A'$) with Si atom sitting on the top and a quasi-planar form **12n.4** (C_1, ^1A), which is constructed by attaching the single Si into an external position of B_{12}[55,59] are also located as the local minima with energy separations of 4 and 11 kcal/mol, respectively.

In the negatively charged state, the anionic $B_{12}Si^-$ ground state **12a.1** (C_s, $^2A'$) possesses the same shape as its neutral counterpart **12n.2**. An elongated quasi-planar **12a.2** (C_1, ^2A), where one peripheral B atom of the B_{13} frame[55] is actually replaced by Si, is found to be the second-lying isomer of $B_{12}Si^-$ with relative energy of 10 kcal/mol. Substitution of one B of the B_{13} cluster[55] by the single Si element at another position and addition of one Si into the B_{12} framework[55,59] continue to form the next isomers **12a.3** (C_1, ^2A) and **12a.4** (C_1, ^2A), being 10 and 11 kcal/mol higher in energy than **12a.1**, respectively.

$B_{13}Si$ and $B_{13}Si^-$. Various structures of the $B_{13}Si$ are located including a hexagonal bipyramid **13n.1** (C_s, $^2A''$), which is generated by doping one Si into the three hexagonal subunits B_{13}^-.[55] A 3D structure **13n.2** (C_{2v}, $^2A_1$) in which one B atom at the apex position of the B_{14} fullerene cage composed of two seven-membered rings[60] is substituted by the Si-atom is also located with 8 kcal/mol higher in energy. The others include two convex forms **13n.3** (C_1, ^2A) and **13n.4** (C_s, $^2A'$), where the Si impurity replaces one peripheral B atom at various positions of the B_{14} skeleton[61] with the relative energies of 19 and 20 kcal/mol, respectively.

The anion **13a.1** (C_s, $^1A'$) keeps the geometry of its neutral counterpart **13n.1**, and becomes the ground state of the anionic $B_{13}Si^-$ clusters. For the second most stable form, at the PBE/6-311+G(d) level, the low-spin structure **13a.3** (C_1, ^1A) is constructed by adding the Si into another external position of anionic elongated quasi-planar form[58] of B_{13}^-. However, our G4 calculated results point out that the configuration **13a.2** (C_{2v}, $^1A_1$), being the corresponding anion of **13n.2**, is the second lowest-lying isomer, and **13a.3** is the third one with energy gaps of 3 and 11 kcal/mol, respectively. The other convex form **13a.4** (C_s, $^1A'$) is also located, being 11 kcal/mol higher in energy as compared to **13a.1**.

$B_{14}Si$ and $B_{14}Si^-$. For $B_{14}Si$, in the lowest-lying configuration **14n.1** (C_s, $^1A'$), the single Si atom is doped into the convex form of B_{14} cluster[58] to bridge with two peripheral B neighbors. The second-lying isomer **14n.2** (C_1, ^1A) is generated by adding the Si into the elongated structure that was reported to be the global minima of the B_{14} at the B3LYP/6-311+G(d) level (in ref 60), and come out to be 8 kcal/mol higher in energy than **14n.1**. The other elongated geometry **14n.3** (C_1, ^1A) and convex form **14n.4** (C_s, $^1A'$) are also located, being about 12 kcal/mol less stable than **14n.1**.

Concerning the anion $B_{14}Si^-$, our G4 calculations result in the ground state (C_s, $^2A''$) **14a.1** that corresponds to the anion of **14n.1**. The structure **14a.2** (C_s, $^2A''$) having the same shape of the neutral counterpart **14n.3** is less stable with a small energy separation of 3 kcal/mol. The next lower-lying convex isomer **14a.3** (C_s, $^2A''$) is also found to be quite stable, being at 4 kcal/mol. The other convex structure **14a.4** (C_1, ^2A) has an energy level at 5 kcal/mol.

In general, on the basis of the structural features of the most stable forms considered above, the grown mechanism of the singly silicon-doped boron clusters B_nSi can be established as follows:

(i) Clusters B_nSi with even number of B atoms can be formed by adding the Si-atom into the B_n frameworks.
i(i) Clusters B_nSi with odd number of B atoms can be formed by substituting one of B atoms of the B_{n+1} frameworks by the Si dopant.

This can be understood by the high thermodynamic stability of the closed-shell pure boron parents B_n with n = 8, 10, 12, and 14.[55,60,61]

3.2. Relative Stability of Clusters. Evaluation of the relative stability of clusters is based on the average binding energy (E_b) and the second-order difference in the total energies (Δ^2E), which can be defined as follows:

$$E_b(B_nSi) = [nE(B) + E(Si) - E(B_nSi)]/(n + 1) \quad (1)$$

$$E_b(B_nSi^-) = [nE(B) + E(Si^-) - E(B_nSi^-)]/(n + 1) \quad (2)$$

$$\Delta^2E(B_nSi) = E(B_{n-1}Si) + E(B_{n+1}Si) - 2E(B_nSi) \quad (3)$$

$$\Delta^2E(B_nSi^-) = E(B_{n-1}Si^-) + E(B_{n+1}Si^-) - 2E(B_nSi^-) \quad (4)$$

where $E(B)$, $E(Si)$, and $E(Si^-)$ are total energies of the B atom, Si-atom, and the charged Si^-, respectively. $E(B_nSi)$, $E(B_nSi^-)$, $E(B_{n-1}Si)$, $E(B_{n-1}Si^-)$, $E(B_{n+1}Si)$, and $E(B_{n+1}Si^-)$ are total energies of the clusters B_nSi, $B_{n-1}Si$, and $B_{n+1}Si$ at the neutral and anionic states, respectively. All of these relative values are obtained from G4 total energies.

It can be seen in Figure 4a, Table 1 and Table 3 (see also ref 37) that the average binding energies are consistently and smoothly increased with increasing boron atom number. The E_b values increase rapidly from BSi to B_8Si and slightly from B_9Si to $B_{14}Si$. While the highest E_b value at the neutral state is found for $B_{14}Si$, $B_{13}Si^-$ reveals the highest one in the series of anions considered.

To gain more insight into relative stability of systems, the second-order difference in energies (Δ^2E) is examined. The Δ^2E plot in Figure 4b consistently shows the even−odd oscillation in which the closed-shell systems exhibit maximum peaks, whereas open-shell systems have minimum peaks. The B_8Si and B_7Si^- are characterized by the highest Δ^2E value in the cases of neutrals and anions, respectively, and they are expected as the enhanced stable species in this series of silicon-doped boron.

To consider the kinetic stability of the $B_nSi^{0/-}$ clusters, the HOMO−LUMO gaps (HLG) of the closed-shell systems are

DOI: 10.1021/acs.jpca.6b00847
J. Phys. Chem. A 2016, 120, 3623−3633

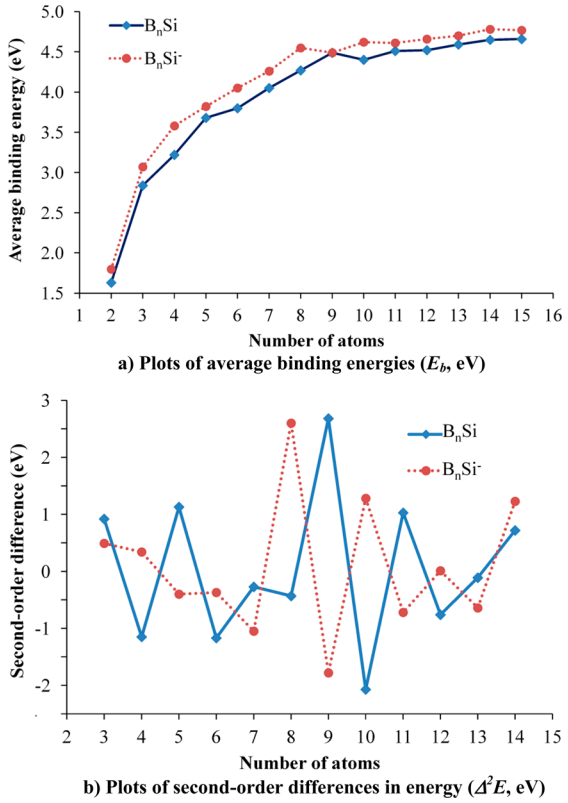

Figure 4. Average binding energy (E_b, eV) (a) and second-order differences in energy (Δ^2E, eV) (b) of the $B_nSi^{0/-}$ clusters (n = 8−14) using the composite G4 approach.

computed using PBE/6-311+G(d) level and displayed in Table 1. The largest value of 4.3 eV is found for B_8Si neutral in the series of clusters selected. This indicates that B_8Si also has a high kinetic stability.

3.3. Vertical (VDE) and Adiabatic (ADE) Detachment Energies. The adiabatic electron detachment energies (ADEs) can be used to evaluate stability of an anionic species. A stable anion with respect to electron ejection is obviously characterized by a high ADE value, whereas a low ADE suggests reluctance of the neutral counterpart to capture an electron. The values for both quantities:

$$\mathrm{ADE} = E(\text{ground state of a neutral}) - E(\text{ground state of an anion})$$

$$\mathrm{VDE} = E(\text{neutral at the geometry of an anionic ground state}) - E(\text{ground state of an anion})$$

are obtained from PBE/6-311+G(d) and G4 calculations and given in Table 2. The differences in ADE values of B_nSi^- derived from both methods are rather small and the largest gap of 0.33 eV was observed for $B_{12}Si^-$. The difference between the ADE and VDE values for species B_nSi^- with n = 9−14, in which the geometries of neutrals and anions are similar, are small. The largest gap of 3.37 eV is found for B_8Si^-. This can be understood on the basis of geometrical change in going from the 3D neutral **8n.1** (C_{7v}) to the 2D anion **8a.1** (C_{2v}). For $B_{12}Si^-$, although geometry also changes from the 3D **12n.1** (C_{3v}) to the 2D **12a.1** (C_s), both ADE and VDE values of this species are close to each other. This can be explained from the fact of that the corresponding neutral structure **12n.2** of the anionic ground state **12a.1** is quite stable and is only 3 kcal/mol less stable than **12n.1**.

Table 2. Adiabatic (ADE) and Vertical (VDE) Detachment Energies (eV) of the Anionic B_nSi^- Clusters (n = 8−14) Using Both PBE/6-311+G(d) and G4 Calculations

	ADE (eV)		VDE (eV)
anions	G4	PBE	PBE
8a.1 (C_{2v}, $^2A_2$)	1.36	1.51	4.88
9a.1 (C_s, $^1A'$)	3.56	3.30	3.49
10a.1 (C_s, $^2A'$)	2.40	2.29	2.42
11a.1 (C_1, ^1A)	2.99	2.78	3.54
11a.2 (C_1, ^1A)	2.97	2.75	2.94
12a.1 (C_s, $^2A'$)	2.82	3.15	3.14
13a.1 (C_s, $^1A'$)	3.18	3.10	3.16
14a.1 (C_s, $^2A''$)	3.03	2.92	3.00

In addition, the detachment energies of the closed-shell anions B_nSi^- with n = 9, 11, and 13 are, as expected, consistently higher than those of the open-shell systems.

3.4. Heats of Formation and Dissociation Energies (D_e). Our previous study on small silicon-doped boron clusters B_nSi with n up to 7[37] showed that the heat of formation of BSi at 298 K obtained from the G4 method is in line with the experimental value determined by using Knudsen cell mass spectrometry and the thermal functions based on a calculated frequency of 772 cm^{-1} for BSi.[35] Therefore, the G4 approach was used in this report to calculate heats of formation of the global minima of the neutral and anionic B_nSi clusters. As there is no available experimental results for the B_nSi sizes considered in the present work, the calculated results given in Table 3 provide us with a consistent and reliable predicted values for thermochemical parameters for these clusters. These computed values are subsequently used to study the thermodynamic stability of clusters.

We also calculated the dissociation energies of the clusters to evaluate further their thermodynamic stability. D_e values obtained from total G4 energies are presented in Table 4. Dissociation energies of the neutral B_nSi clusters from the channel (1) $B_nSi \rightarrow B_n + Si$ are found to be smaller than those from the channel (2) $B_nSi \rightarrow B_{n-1}Si + B$. These calculated results suggest that B_nSi neutrals tend to be established by doping one Si-atom into the pure B_n frameworks, except for B_9Si.

The D_e values of B_9Si from the channel (2) $B_9Si \rightarrow B_8Si + B$ (83 kcal/mol) is smaller than that from channel (1) $B_9Si \rightarrow B_9 + Si$ (104 kcal/mol). Additionally, dissociation energies of B_8Si from all two channels are significantly high in comparison to those of larger clusters. These results indicate that B_8Si possesses a peculiarly high thermodynamic stability. For the B_nSi^- clusters, due to the fact that D_e values from the channel (4) $B_nSi^- \rightarrow B_n^- + Si$ are the smallest as compared to those from remaining channels, the anions B_nSi^- tend to be decomposed to smaller B_n^- clusters plus Si atom. Similarly, with the highest dissociation energies, B_9Si^- and $B_{13}Si^-$ also exhibit an enhanced stability. These observations are reasonably consistent with the above predictions.

3.5. Chemical Bonding and Aromaticity. The high symmetry geometry and thermodynamic stability of the B_8Si are rather intriguing, and thus deserve a further analysis of its electronic structure and chemical bonding. Aromaticity[46] is often pointed out as an typical characteristic for pure and impure boron clusters, which has extensively been discussed in

DOI: 10.1021/acs.jpca.6b00847
J. Phys. Chem. A 2016, 120, 3623−3633

Table 3. Total Atomization Energies (TAE) (kcal/mol) and Heats of Formation at 0 K [ΔH_f(0 K)] and 298 K [ΔH_f (298 K)] (kcal/mol) of the Neutral B_nSi and Anionic B_nSi^- Clusters (n = 8−14) Using the G4 Method

	TAE (0 K)		ΔH_f (0 K)		ΔH_f (298 K)	
structures	G4	exptl.	G4	exptl.	G4	exptl.
1n.1 ($C_{\infty v}$, $^4\Sigma^-$)	74.18[37]	74.57 ± 2.87[35]	167.1[37]	165.87 ± 3.35[35]	168.1[37]	166.83 ± 3.35[35]
8n.1 (C_{7v}, $^1A_1$)	932.0		256.0		258.1	
8a.1 (C_{2v}, $^2A_2$)	963.5		224.5		227.0	
9n.1 (C_1, ^2A)	1014.6		308.5		310.6	
9a.1 (C_s, $^1A'$)	1096.7		226.4		228.5	
10n.1 (C_s, $^1A'$)	1144.9		313.3		315.2	
10a.1 (C_s, $^2A'$)	1200.3		257.9		260.0	
11n.1 (C_1, ^2A)	1251.5		341.8		344.2	
11a.1 (C_1, ^1A)	1320.5		272.8		275.4	
11a.2 (C_1, ^1A)	1319.8		273.5		275.8	
12n.1 (C_{3v}, $^1A_1$)	1375.4		353.0		355.1	
12a.1 (C_s, $^2A'$)	1440.4		288.0		290.6	
13n.1 (C_s, $^2A''$)	1501.9		361.6		364.4	
13a.1(C_s, $^1A'$)	1575.2		288.3		291.0	
14n.1 (C_s, $^1A'$)	1611.8		386.8		389.7	
14a.1 (C_s, $^2A''$)	1681.8		316.8		320.1	

Table 4. Dissociation Energies (D_e, kcal/mol) for Various Fragmentation Channels of $B_nSi^{0/-}$ (n = 8−14) (G4 Calculations)[a]

neutrals	D_e (1)	D_e (2)	anions	D_e (3)	D_e (4)	D_e (5)	D_e (6)
8n.1	134.6	144.3	**8a.1**	155.5	93.6	178.0	92.3
9n.1	104.3	82.6	**9a.1**	175.8	120.8	166.9	133.2
10n.1	104.6	130.3	**10a.1**	149.4	93.3	187.9	103.6
11n.1	95.7	106.5	**11a.1**	154.2	85.5	177.8	120.2
			11a.2	153.5	84.8	177.2	119.5
12n.1	85.3	124.0	**12a.1**	139.8	95.6	191.2	119.9
13n.1	112.4	129.0	**13a.1**	175.2	123.0	204.6	134.8
14n.1	87.1	117.9	**14a.1**	146.6	97.4	190.1	117.7

[a](**1**) $B_nSi \rightarrow B_n + Si$; (**2**) $B_nSi \rightarrow B_{n-1}Si + B$; (**3**) $B_nSi^- \rightarrow B_n + Si^-$; (**4**) $B_nSi^- \rightarrow B_n^- + Si$; (**5**) $B_nSi^- \rightarrow B_{n-1}Si + B^-$; (**6**) $B_nSi^- \rightarrow B_{n-1}Si^- + B$.

the literature.[62−65] The electron localization function (ELF) is an indicator that is effectively used to probe the electron distribution of compounds, including novel organic compounds and atomic clusters.[66] The topological analysis of the ELF[47] shows that a structure whose ELF isosurface has a high bifurcation value exhibits an aromatic character, whereas a structure possessing a low bifurcation ELF value is not aromatic.

With its hypercoordinated structure, the perfect planar wheel **8n.3** (D_{8h}, $^1A_{1g}$) has been analyzed in some previous studies.[56,67−69] The perfect octagon **8n.3** has been shown to possess a double aromaticity with three delocalized π-orbitals and three delocalized σ-radial bonds. Herein, we would focus on the bipyramid **8n.1**.

Figure 5a points out a good electron delocalization over the entire structure of **8n.1**. The corresponding ELF map also depicts the presence of seven distinct disynaptic basins between the peripheral atoms of the heptagonal bipyramid (C_{7v}, $^1A_1$), in which each basin contains ∼2.8 electrons. More importantly, the bifurcation value of ELF isosurface of **8n.1** is high. A complete separation of basins is only observed at a high value of ELF = 0.85. In this regard, the neutral B_8Si **8n.1** can be regarded as possessing a certain aromaticity.

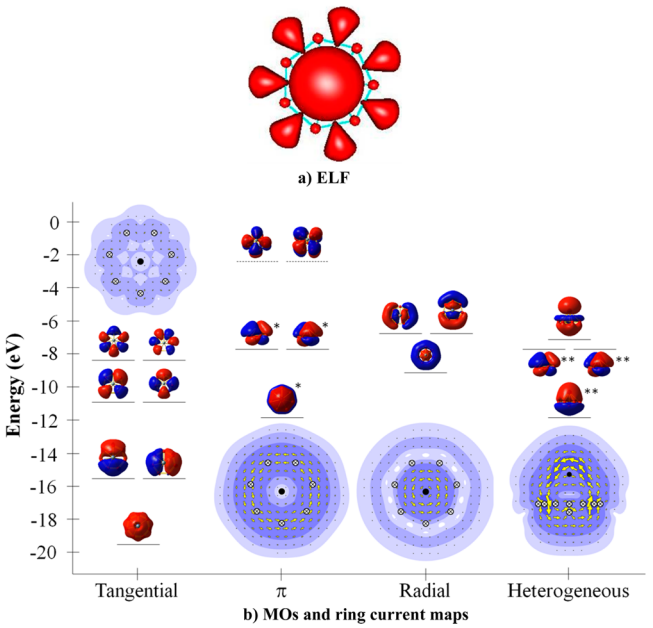

Figure 5. Characteristics of the neutral B_8Si **8n.1** (C_{7v}). The electron localization function (ELF) isosurface (a) at bifurcation value of 0.85 (using the PBE/6-311+G(d) computations), and the molecular orbitals (b) categorized into tangential, π, radial and heterogeneous sets and their ring current maps, correspondingly. The "**" MOs are reused from the "*" MOs.

Let us note a relationship between the aromatic character of the neutral B_8Si and the anion B_7Si^-, which was reported in a recent theoretical study.[37] Similar to B_7Si^-, B_8Si contains six delocalized valence π-electrons and six delocalized σ-electrons that fully occupy the orbitals HOMO−2, HOMO−2′ and HOMO−6 for the former, and HOMO, HOMO′ and HOMO−4 for the latter. Based on the Hückel's electron count,[70] which was classically applied to delocalized π-electrons, but can also be used for delocalized σ-electrons, this species turns out to be doubly (π and σ) aromatic ($4N + 2$ electrons, N = 1).

DOI: 10.1021/acs.jpca.6b00847
J. Phys. Chem. A 2016, 120, 3623−3633

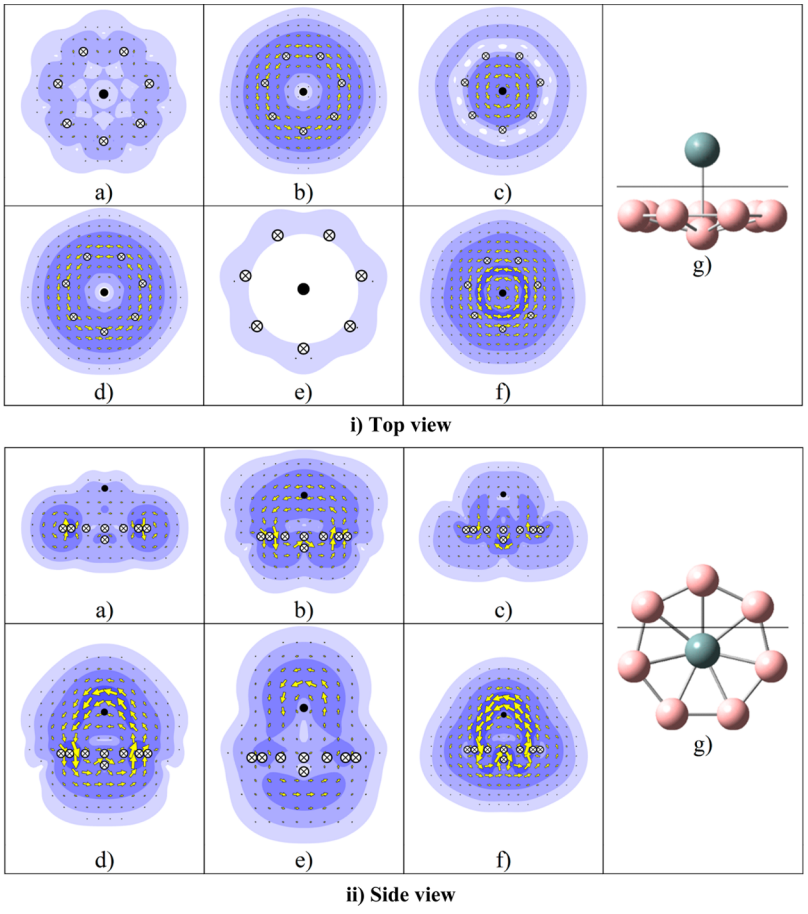

Figure 6. Orbital contributions to the current density in B_8Si from (i) the top view and (ii) the side view. The sum of orbital contributions of (a) 14 electrons in the tangential set; (b) 6 electrons in the π set; (c) 6 electron in the radial set; (d) 8 electrons in the heterogeneous set; (e) 2 electrons in HOMO−1; and (f) the total electron of the B_8Si; (g) the geometry of B_8Si with the black lines corresponding to the plane in which the ring current maps are calculated.

As in the case of the Mg-doped clusters B_7Mg^- and B_8Mg^- that were shown to have umbrella-like structures,[22] the electrons of B_7Si^- and B_8Si could be separated into three different types, namely tangential electrons, radial electrons, and π bonding (displayed in Figure S4 of the Supporting Information (SI) files and Figure 5b, respectively). These three types of electrons reinforce the boron cycles from the pure B_7^- and B_8 cycles.[55,58] Each series of electrons leads to an different aromatic character.

From a different perspective, the set of π MOs, and the HOMO−1 of the anion B_7Si^- are classified as a heterogeneous set, because they enhance the bonding between the Si atom and the boron cycles (Figure S4 of the ESI). Similarly, the set of π MOs and the HOMO−1 of the neutral B_8Si can also be classified as a heterogeneous set (Figure 5b). To further confirm the aromatic character of these systems, the magnetic ring current maps for each form of these four sets from top view and side view are calculated. In the ring current model of magnetic response, the aromaticity/antiaromaticity is associated with diatropic/paratropic ring currents that are presented by counterclockwise/clockwise circulations, respectively.

The magnetic ring current maps for B_8Si presented in Figure 6i (the top view) and Figure 6ii (the side view) are calculated in the plane y = 0.5 Å and z = 0.5 Å, respectively. The black line indicates the plane y = 0.5 Å in Figure 6i(g) and z = 0.5 Å in Figure 6ii(g). For the anion B_7Si^-, the magnetic current density maps are similarly plotted in Figure S5i (the top view) and Figure S5ii (the side view) in the plane y = 0.5 Å [Figure S5i(g)] and z = 0.5 Å [Figure S5ii(g) of the ESI file].

The ring current maps for both anionic B_7Si^- and neutral B_8Si are remarkably similar. While the radial set of electrons contributes primarily to the top view aromaticity, which corresponds to an aromaticity of the boron cycle, the π set of electrons joins into both the top view and the side view aromaticity. The HOMO−1 of both structures B_7Si^- and B_8Si show no contribution to the top view ring current maps, but they contribute completely into the side view ring current maps. Therefore, the electrons in the HOMO−1 and the π set combine together to form a heterogeneous set that describes the bonding between the dopant Si and the boron cycle. In other words, the electrons in both structures B_7Si^- and B_8Si achieve a triple aromaticity, including a π aromaticity, a radial aromaticity and a heterogeneous aromaticity, all in three-dimensional distribution.

4. CONCLUDING REMARKS

In this theoretical study, we systematically explored the following sizes of silicon-doped boron clusters B_nSi with n = 8−14, in both neutral and anionic charge states using quantum chemical calculations. The global minima of the clusters selected were determined on the basis of the energies obtained using the composite G4 model. Thermochemical parameters of the $B_nSi^{0/-}$ clusters such as total atomization energies,

DOI: 10.1021/acs.jpca.6b00847
J. Phys. Chem. A 2016, 120, 3623−3633

enthalpies of formation at 0 and 298 K, average binding energies, dissociation energies, etc., were predicted by using the G4 energies.

The growth behavior for the singly silicon-doped boron clusters $B_nSi^{0/-}$ with n = 1−14 (n = 8−14 were studied in the current work, and n = 1−7 were reported in ref 37) can be established as follows:

(i) Most of the ground state structures of $B_nSi^{0/-}$ clusters tend to be formed by substituting B atom by Si atom or attaching one Si impurity into the parent boron clusters.

(ii) Si tends to prefer a peripheral position of the boron frameworks with low coordination numbers, although in B_7Si^-, B_8Si, and $B_{12}Si$ isomers, Si possesses a high coordination number.

Our calculated results also pointed out that the species B_8Si, B_9Si^-, $B_{10}Si$, and $B_{13}Si^-$ are characterized by an enhanced stability with high average binding energies, second-order difference in energies, and dissociation energies. An analysis of the MOs, ELF, and magnetic ring current maps suggested that the peculiar stability of the closed-shell species B_8Si can be rationalized in terms of a triple aromaticity.

■ ASSOCIATED CONTENT

Supporting Information

The Supporting Information is available free of charge on the ACS Publications website at DOI: 10.1021/acs.jpca.6b00847.

Table containing the Cartesian coordinates of the lowest-lying isomers $B_nSi^{0/-}$ considered. Figures displaying the shapes of low-lying isomers $B_nSi^{0/-}$, molecular orbitals, and ring current maps of B_7Si^-. (PDF)

■ AUTHOR INFORMATION

Corresponding Author

*E-mail: minh.nguyen@kuleuven.be; Telephone number: +32−16-327361.

Notes

The authors declare no competing financial interest.

■ ACKNOWLEDGMENTS

D.T.T.M. thanks the Vietnam Ministry of Education and Training for a doctoral scholarship (911 program). The work at ICST is supported by the Department of Science and Technology of Ho Chi Minh City. TBT thanks the FWO-Vlaanderen for a postdoctoral fellowship. We are also grateful to Tran Dieu Hang for her efficient assistance. MTN is indebted to the KU Leuven Research Council (GOA programs) for continuing support.

■ REFERENCES

(1) Boustani, I. Towards Novel Boron Nanostructrural Materials. *Chem. Model.* **2011**, *8*, 1−44.

(2) Dash, B. P.; Satapathy, R.; Maguire, J. A.; Hosmane, N. S. Polyhedral Boron Clusters in Materials Science. *New J. Chem.* **2011**, *35*, 1955−1972.

(3) Grimes, R. N. Viewpoints: Chemists on Chemistry Boron Clusters Come of Age. *J. Chem. Educ.* **2004**, *81*, 657−672.

(4) Plesek, J. Potential Applications of the Boron Cluster Compounds. *Chem. Rev.* **1992**, *92*, 269−278.

(5) Tai, T. B.; Nguyen, M. T. Electronic Structure and Photoelectron Spectra of B_n with n = 26−29: An Overview of Structural Characteristics and Growth Mechanism of Boron Clusters. *Phys. Chem. Chem. Phys.* **2015**, *17*, 13672−13679.

(6) Arvanitidis, A. G.; Tai, T. B.; Nguyen, M. T.; Ceulemans, A. Quantum Rules for Planar Boron Nanoclusters. *Phys. Chem. Chem. Phys.* **2014**, *16*, 18311−18318.

(7) Feng, X.-J.; Zhao, L.-X.; Cao, T.-T.; Lei, Y.-M.; Luo, Y.-H. Theoretical Prediction of Structural and Magnetic Properties of Small Rhenium Boride Clusters. *Phys. B* **2008**, *403*, 4323−4327.

(8) Böyükata, M.; Güvenç, Z. B. Density Functional Study of AlB_n Clusters for n = 1−14. *J. Alloys Compd.* **2011**, *509*, 4214−4234.

(9) Jia, J.; Li, X.; Li, Y.; Ma, L.; Wu, H.-S. Density Functional Theory Investigation on the Structure and Stability of Sc_2B_n (n = 1−10) Clusters. *Comput. Theor. Chem.* **2014**, *1027*, 128−134.

(10) Cheng, S.-B.; Berkdemir, C.; Castleman, A. W. Observation of D-P Hybridized Aromaticity in Lanthanum-Doped Boron Clusters. *Phys. Chem. Chem. Phys.* **2014**, *16*, 533−539.

(11) Gu, J.; Wang, C.; Cheng, Y.; Zhang, L.; Yang, X. Probing the Structural and Electronic Properties of Boron Cluster Anions Doped with One or Two Aluminum Atoms. *Comput. Theor. Chem.* **2014**, *1049*, 67−74.

(12) Tam, N. M.; Pham, H. T.; Duong, L. V.; Pham-Ho, M. P.; Nguyen, M. T. Fullerene-like Boron Clusters Stabilized by an Endohedrally Doped Iron Atom: B_nFe with n = 14, 16, 18 and 20. *Phys. Chem. Chem. Phys.* **2015**, *17*, 3000−3003.

(13) Jia, J.; Ma, L.; Wang, J.-F.; Wu, H.-S. Structures and Stabilities of ScB_n (n = 1−12) Clusters: An Ab Initio Investigation. *J. Mol. Model.* **2013**, *19*, 3255−3261.

(14) Yao, J.-G.; Wang, X.-W.; Wang, Y.-X. A Theoretical Study on Structural and Electronic Properties of Zr-Doped B Clusters: ZrB_n (n = 1−12). *Chem. Phys.* **2008**, *351*, 1−6.

(15) Feng, X. J.; Luo, Y. H. Structure and Stability of Al-Doped Boron Clusters by the Density-Functional Theory. *J. Phys. Chem. A* **2007**, *111*, 2420−2425.

(16) Romanescu, C.; Galeev, T. R.; Li, W.-L.; Boldyrev, A. I.; Wang, L.-S. Aromatic Metal-Centered Monocyclic Boron Rings: Co©B_8^- and Ru©B_9^-. *Angew. Chem., Int. Ed.* **2011**, *50*, 9334−9337.

(17) Romanescu, C.; Galeev, T. R.; Li, W.-L.; Boldyrev, A. I.; Wang, L.-S. Geometric and Electronic Factors in the Rational Design of Transition-Metal-Centered Boron Molecular Wheels. *J. Chem. Phys.* **2013**, *138*, 134315.

(18) Li, W. L.; Ivanov, A. S.; Federič, J.; Romanescu, C.; Černušák, I.; Boldyrev, A. I.; Wang, L.-S. On the Way to the Highest Coordination Number in the Planar Metal-Centred Aromatic Ta©B_{10}^- Cluster: Evolution of the Structures of TaB_n^- (n = 3−8). *J. Chem. Phys.* **2013**, *139*, 104312.

(19) Romanescu, C.; Galeev, T. R.; Li, W.-L.; Boldyrev, A. I.; Wang, L.-S. Transition-Metal-Centered Monocyclic Boron Wheel Clusters (M©B_n): A New Class of Aromatic Borometallic Compounds. *Acc. Chem. Res.* **2013**, *46*, 350−358.

(20) Popov, I. A.; Li, W.-L.; Piazza, Z. A.; Boldyrev, A. I.; Wang, L.-S. Complexes between Planar Boron Clusters and Transition Metals: A Photoelectron Spectroscopy and Ab Initio Study of CoB_{12}^- and RhB_{12}^-. *J. Phys. Chem. A* **2014**, *118*, 8098−8105.

(21) Pham, H. T.; Nguyen, M. T. Effects of Bimetallic Doping on Small Cyclic and Tubular Boron Clusters: B_7M_2 and $B_{14}M_2$ Structures with M = Fe, Co. *Phys. Chem. Chem. Phys.* **2015**, *17*, 17335−17345.

(22) Reber, A. C.; Khanna, S. N. Electronic Structure, Stability, and Oxidation of Boron-Magnesium Clusters and Cluster Solids. *J. Chem. Phys.* **2015**, *142*, 054304.

(23) Wu, J.; Ma, W.; Tang, D.; Jia, B.; Yang, B.; Liu, D.; Dai, Y. Thermodynamic Description of Si-B Binary System. *Procedia Eng.* **2012**, *31*, 297−301.

(24) Dirkx, R. R.; Spear, K. E. Optimization of Thermodynamic Data for Silicon Borides. *CALPHAD: Comput. Coupling Phase Diagrams Thermochem.* **1987**, *11*, 167−175.

(25) Vlasse, M.; Slack, G. A.; Garbauskas, M.; Kasper, J. S.; Viala, J. C. The Crystal Structure of SiB6. *J. Solid State Chem.* **1986**, *63*, 31−45.

(26) Vlasse, M.; Viala, J. C. The Boron-Silicon Solid Solution: A Structural Study of the $SiB_{\sim 36}$ Composition. *J. Solid State Chem.* **1981**, *37*, 181−188.

DOI: 10.1021/acs.jpca.6b00847
J. Phys. Chem. A 2016, 120, 3623−3633

(27) Armas, B.; Male, G.; Salanoubat, D.; Chatillon, C.; Allibert, M. Determination Diagram of the Boron-Rich Side of the B-Si Phase. *J. Less-Common Met.* **1981**, *82*, 245−254.
(28) Ito, H.; Kosaka, Y.; Nonoyama, K.; Sasaki, Y.; Sawamura, M. Synthesis of Optically Active Boron-Silicon Bifunctional Cyclopropane Derivatives through Enantioselective Copper(I)-Catalyzed Reaction of Allylic Carbonates with a Diboron Derivative. *Angew. Chem., Int. Ed.* **2008**, *47*, 7424−7427.
(29) Colton, E. On the Boron-Silicon Reaction. *J. Inorg. Nucl. Chem.* **1961**, *17*, 108−111.
(30) Tremblay, R.; Angers, R. Preparation of High Purity SiB_4 by Solid-State Reaction between Si and B. *Ceram. Int.* **1989**, *15*, 73−78.
(31) Imai, M.; Kimura, T.; Sato, K.; Hirano, T. Single-Crystal Growth and Electrical Properties of B_nSi (n = 18). *J. Alloys Compd.* **2000**, *306*, 197−202.
(32) Zaitsev, A. I.; Kodentsov, A. A. Thermodynamic Properties and Phase Equilibria in the Si-B System. *J. Phase Equilib.* **2001**, *22*, 126−135.
(33) Imai, Y.; Mukaida, M.; Ueda, M.; Watanabe, A. Band-Calculation of the Electronic Densities of States and the Total Energies of Boron-Silicon System. *J. Alloys Compd.* **2002**, *347*, 244−251.
(34) Tam, N. M.; Tai, T. B.; Nguyen, M. T. Thermochemical Parameters and Growth Mechanism of the Boron- Doped Silicon Clusters, Si_nB^q with n = 1−10 and q = − 1, 0, + 1. *J. Phys. Chem. C* **2012**, *116*, 20086−20098.
(35) Viswanathan, R.; Schmude, R. W.; Gingerich, K. A. Thermochemistry of BSi(g), BSi_2(g), and BSi_3(g). *J. Phys. Chem.* **1996**, *100*, 10784−10786.
(36) Davy, R.; Skoumbourdis, E.; Dinsmore, D. Structure, Energies, Vibrational Spectra and Reactions of the Boron−Silicon Cluster Molecules B_2Si, BSi_2 and B_2Si_2. *Mol. Phys.* **2005**, *103*, 611−619.
(37) Tai, T. B.; Kadłubański, P.; Roszak, S.; Majumdar, D.; Leszczynski, J.; Nguyen, M. T. Electronic Structures and Thermochemical Properties of the Small Silicon-Doped Boron Clusters B_nSi (n = 1−7) and Their Anions. *ChemPhysChem* **2011**, *12*, 2948−2958.
(38) Tai, T. B.; Nguyen, M. T. A Stochastic Search for the Structures of Small Germanium Clusters and Their Anions: Enhanced Stability by Spherical Aromaticity of the Ge_{10} and Ge_{12}^{2-} Systems. *J. Chem. Theory Comput.* **2011**, *7*, 1119−1130.
(39) Perdew, J. P.; Burke, K.; Ernzerhof, M. Generalized Gradient Approximation Made Simple. *Phys. Rev. Lett.* **1996**, *77*, 3865−3868.
(40) Stevens, W. J.; Krauss, M.; Basch, H.; Jasien, P. G. Relativistic Compact Effective Potentials and Efficient, Shared-Exponent Basis Sets for the Third-, Fourth-, and Fifth-Row Atoms. *Can. J. Chem.* **1992**, *70*, 612−630.
(41) Krishnan, R.; Binkley, J. S.; Seeger, R.; Pople, J. A. Self-Consistent Molecular Orbital Methods. XX. A Basis Set for Correlated Wave Functions. *J. Chem. Phys.* **1980**, *72*, 650.
(42) Curtiss, L. A.; Redfern, P. C.; Raghavachari, K. Gaussian-4 Theory. *J. Chem. Phys.* **2007**, *126*, 084108.
(43) Peterson, K. A.; Xantheas, S. S.; Dixon, D. A.; Dunning, T. H. Predicting the Proton Affinities of H_2O and NH_3. *J. Phys. Chem. A* **1998**, *102*, 2449−2454.
(44) Karton, A.; Martin, J. M. L. Heats of Formation of Beryllium, Boron, Aluminum, and Silicon Re-Examined by Means of W4 Theory. *J. Phys. Chem. A* **2007**, *111*, 5936−5944.
(45) Curtiss, L. A.; Raghavachari, K.; Redfern, P. C.; Pople, J. A. Assessment of Gaussian-2 and Density Functional Theories for the Computation of Enthalpies of Formation. *J. Chem. Phys.* **1997**, *106*, 1063−1073.
(46) Fowler, J. E.; Ugalde, J. M. The Curiously Stable Cluster and Its Neutral and Anionic Counterparts: The Advantages of Planarity. *J. Phys. Chem. A* **2000**, *104*, 397−403.
(47) Silvi, B.; Savin, A. Classification of Chemical Bonds Based on Topological Analysis of Electron Localization Functions. *Nature* **1994**, *371*, 683−686.
(48) Savin, A.; Silvi, B.; Coionna, F. Topological Analysis of the Electron Localization Function Applied to Delocalized Bonds. *Can. J. Chem.* **1996**, *74*, 1088−1096.
(49) Zanasi, R. Coupled Hartree−Fock Calculations of Molecular Magnetic Properties Annihilating the Transverse Paramagnetic Current Density. *J. Chem. Phys.* **1996**, *105*, 1460.
(50) Lazzeretti, P.; Malagoli, M.; Zanasi, R. Electronic Current Density Induced by Nuclear Magnetic Dipoles. *J. Mol. Struct.: THEOCHEM* **1994**, *313*, 299−304.
(51) Guest, M. F.; Bush, I. J.; Van Dam, H. J. J.; Sherwood, P.; Thomas, J. M. H.; Van Lenthe, J. H.; Havenith, R. W. A.; Kendrick, J. The GAMESS-UK Electronic Structure Package: Algorithms, Developments and Applications. *Mol. Phys.* **2005**, *103*, 719−747.
(52) Havenith, R. W. A.; Fowler, P. W. Ipsocentric Ring Currents in Density Functional Theory. *Chem. Phys. Lett.* **2007**, *449*, 347−353.
(53) Lazzeretti, P.; Zanasi, R. SYSMO Package; University of Modena: Modena, Italy, 1980, with additional routines for evaluation and plotting of current densities by Steiner, E.; Fowler, F. W.; Havenith, R. W. A.; and Soncini, A.
(54) Frisch, M.; Trucks, G.; Schlegel, H. et al. *Gaussian 09*, revision: A.02; Gaussian, Inc.: Wallingford, CT, 2009.
(55) Tai, T. B.; Grant, D. J.; Nguyen, M. T.; Dixon, D. A. Thermochemistry and Electronic Structure of Small Boron Clusters (B_n, n = 5−13) and Their Anions. *J. Phys. Chem. A* **2010**, *114*, 994−1007.
(56) Islas, R.; Heine, T.; Ito, K.; Schleyer, P. v R.; Merino, G. Boron Rings Enclosing Planar Hypercoordinate Group 14 Elements. *J. Am. Chem. Soc.* **2007**, *129*, 14767−14774.
(57) Tai, T. B.; Nguyen, M. T. Thermochemical Properties, Electronic Structure and Bonding of Mixed Lithium Boron Clusters (B_nLi, n = 1−8) and Their Anions. *Chem. Phys.* **2010**, *375*, 35−45.
(58) Alexandrova, A. N.; Boldyrev, A. I.; Zhai, H. J.; Wang, L. S. All-Boron Aromatic Clusters as Potential New Inorganic Ligands and Building Blocks in Chemistry. *Coord. Chem. Rev.* **2006**, *250*, 2811−2866.
(59) Kiran, B.; Gopa Kumar, G.; Nguyen, M. T.; Kandalam, A. K.; Jena, P. Origin of the Unusual Stability of B_{12} and B_{13}^+ Clusters. *Inorg. Chem.* **2009**, *48*, 9965−9967.
(60) Cheng, L. B_{14}: An All-Boron Fullerene. *J. Chem. Phys.* **2012**, *136*, 104301.
(61) Tai, T. B.; Tam, N. M.; Nguyen, M. T. Structure of Boron Clusters Revisited, B_n with n = 14−20. *Chem. Phys. Lett.* **2012**, *530*, 71−76.
(62) Mercero, J. M.; Boldyrev, A. I.; Merino, G.; Ugalde, J. M. Recent Developments and Future Prospects of All-Metal Aromatic Compounds. *Chem. Soc. Rev.* **2015**, *44*, 6519−6534.
(63) Moreno, D.; Pan, S.; Zeonjuk, L. L.; Islas, R.; Osorio, E.; Martínez-Guajardo, G.; Chattaraj, P. K.; Heine, T.; Merino, G. B_{18}^{2-}: A Quasi-Planar Bowl Member of the Wankel Motor Family. *Chem. Commun.* **2014**, *50*, 8140−8143.
(64) Jiménez-Halla, J. O. C.; Islas, R.; Heine, T.; Merino, G. B_{19}^-: An Aromatic Wankel Motor. *Angew. Chem., Int. Ed.* **2010**, *49*, 5668−5671.
(65) Martínez-Guajardo, G.; Sergeeva, A. P.; Boldyrev, A. I.; Heine, T.; Ugalde, J. M.; Merino, G. Unravelling Phenomenon of Internal Rotation in B_{13}^+ through Chemical Bonding Analysis. *Chem. Commun.* **2011**, *47*, 6242−62444.
(66) Santos, J. C.; Tiznado, W.; Contreras, R.; Fuentealba, P. Sigma-Pi Separation of the Electron Localization Function and Aromaticity. *J. Chem. Phys.* **2004**, *120*, 1670−1673.
(67) Minyaev, R. M.; Gribanova, T. N.; Starikov, A. G.; Minkin, V. I. Octacoordinated Main-Group Element Centres in a Planar Cyclic B_8 Environment: An Ab Initio Study. *Mendeleev Commun.* **2001**, *11*, 213−214.
(68) Li, S.-D.; Miao, C.-Q.; Guo, J.-C.; Ren, G.-M. Planar Tetra-, Penta-, Hexa-, Hepta-, and Octacoordinate Silicons: A Universal Structural Pattern. *J. Am. Chem. Soc.* **2004**, *126*, 16227−16231.
(69) Bomble, L.; Steinmann, S. N.; Perez-Peralta, N.; Merino, G.; Corminboeuf, C. Bonding Analysis of Planar Hypercoordinate Atoms

DOI: 10.1021/acs.jpca.6b00847
J. Phys. Chem. A 2016, 120, 3623−3633

via the Generalized BLW-LOL. *J. Comput. Chem.* **2013**, *34*, 2242−2248.
(70) Garratt, P. J. *Aromaticity*; Wiley-Interscience: New York, 1986.

DOI: 10.1021/acs.jpca.6b00847
J. Phys. Chem. A 2016, 120, 3623−3633